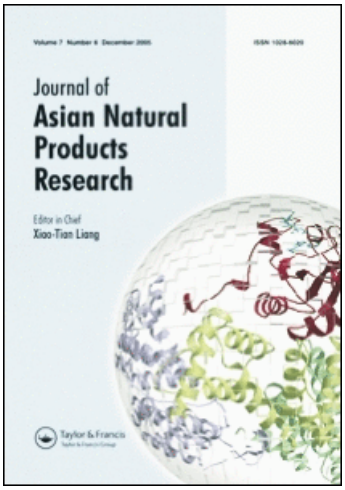

Journal of Asian Natural Products Research
Publication details, including instructions for authors and subscription information:
http://www.informaworld.com/smpp/title~content=t713454007

Effects of PLAB on apoptosis and Smad signal pathway of hypertrophic scar fibroblasts

BO Cao[a]; MENG-CHEN Jiang[a]; ZHI-YONG Lei[a]; SHU-FANG Bai[a]; HONG Chen[a]
[a] Department of Pharmacognosy, Medical College of Chinese People's Armed Police Forces, Tianjin, China

To cite this Article Cao, BO , Jiang, MENG-CHEN , Lei, ZHI-YONG , Bai, SHU-FANG and Chen, HONG(2008) 'Effects of PLAB on apoptosis and Smad signal pathway of hypertrophic scar fibroblasts', Journal of Asian Natural Products Research, 10: 2, 147 — 157
To link to this Article: DOI: 10.1080/10286020701394308
URL: http://dx.doi.org/10.1080/10286020701394308

Journal of Asian Natural Products Research, Vol. 10, No. 2, February 2008, 147–157

Effects of PLAB on apoptosis and Smad signal pathway of hypertrophic scar fibroblasts

BO CAO, MENG-CHEN JIANG, ZHI-YONG LEI, SHU-FANG BAI and HONG CHEN*

Department of Pharmacognosy, Medical College of Chinese People's Armed Police Forces, Tianjin 300162, China

(Received 18 September 2006; revised 9 January 2007; in final form 20 January 2007)

Pseudolaric acid-B (PLAB), a diterpene acid, was isolated from the root and trunk barks of *Pseudolarix kaempferi*. It has shown antifungal and anti-fertility effects and cytotoxic activities in previous studies. Our goals are to study the effects of PLAB on cell proliferation and Smad signal pathway of hypertrophic scar fibroblasts. Our results showed that PLAB induced apoptosis in hypertrophic scar fibroblasts and inhibited cell proliferation of hypertrophic scar fibroblast. MTT assay showed that its IC_{50} value toward hypertrophic scar fibroblasts was $12.9 \pm 1.20\,\mu$mol/L. Furthermore, the results of cell growth curve matched with the above results. Inducing apoptosis by PLAB in hypertrophic scar fibroblast was assessed by various morphological and biochemical characteristics, including cell shrinkage, chromatin condensation, membrane blebbing, formation of apoptotic bodies, and DNA ladder formation. A typical "Sub-G1 peak" was also checked through flow cytometry. The Smad2 and Smad7 mRNA levels of 48-h PLAB treatment were determined by reverse transcription–polymerase chain reaction (RT-PCR) 48 h later. RT-PCR showed that Smad7 mRNA level increased and significant differences were observed between control group and experimental group ($P < 0.05$); While there is no significant difference in Smad2 mRNA between the two groups. Our results showed that PLAB interfered with the microtubule dynamics of tubulin polymerisation and depolymerisation, which results in the inhibition of chromosomal segregation in mitosis and consequently the inhibition of cell division. These results suggest that PLAB inhibits hypertrophic scar fibroblast growth through apoptosis and Smad signal pathway.

Keywords: Pseudolaric acid-B; Hypertrophic scar; Apoptosis; Smad2; Smad7

1. Introduction

Hypertrophic scar is a unique human dermal fibroproliferative disorder that occurs after trauma, inflammation, burns, surgery, and possibly, spontaneously. Although it is not fatal, it is a major cosmetic problem and symptoms like itching and pain can significantly affect the patient's quality of life. The mechanism of hypertrophic scar is still unclear and there is no effective therapy for it. In the last decade more attention has been given to uncover the benefits of natural products in relation to hypertrophic scar. Pseudolaric acid-B (figure 1),

*Corresponding author. Email: chenhongtian06@yahoo.com.cn

Journal of Asian Natural Products Research
ISSN 1028-6020 print/ISSN 1477-2213 online © 2008 Taylor & Francis
http://www.tandf.co.uk/journals
DOI: 10.1080/10286020701394308

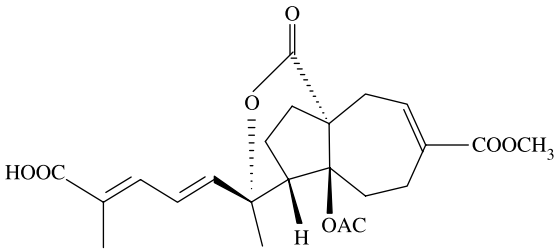

Figure 1. Chemical structure of Pseudolaric acid-B.

a novel diterpene acid, was isolated and identified as the main antifungal constituent from *Pseudolarix kaempferi* Gorden [1,2]. It also showed anti-fertility effects [3,4] and was established as a general cytotoxic agent against P-388 lymphocytic leukaemia, KB carcinoma of the nasopharynx, HT-1080 fibrosarcoma, human breast cancer, human melanoma, human lung cancer, and human colon cancer cells [5,6] *in vitro*. Failure of apoptosis has been postulated to cause the hypercellularity and thus excess scar-tissue formation of hypertrophic scars [7]. A dysregulation in Fas-mediated apoptosis that normally occurs during the process of wound healing may be an important mechanism by which keloids arise and that transforming growth factor (TGF)-β1 is an important factor responsible for this resistance [8].

For the first time, our results herein show that PLAB inhibited hypertrophic scar fibroblast growth through apoptosis and Smad signal pathway.

2. Results and discussion

2.1 Effect of PLAB on growth of hypertrophic scar fibroblasts

Figure 2 showed the growth of fibroblast was inhibited by PLAB in different concentration (2–16 μmol/L). The inhibition rate of fibroblast increased up to 71.25% treated with 32 μmol/L PLAB. The IC_{50} value was 12.9 ± 1.2 μmol/L.

Furthermore, the results of cell growth curve of FB matched the results above (figure 3). The number of control cells increased over 30 times after 6 days, whereas the number of cells

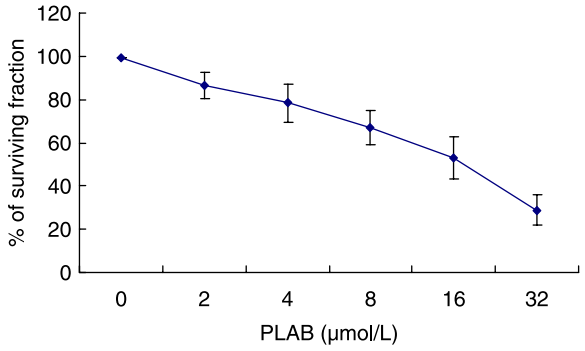

Figure 2. Effect of PLAB cytotoxicity. FB cells were exposed to increasing concentrations of PLAB (2–32 μmol/L) for 96 h. Surviving fraction was determined by MTT assay. Data were given as mean of triplicate values ± SD.

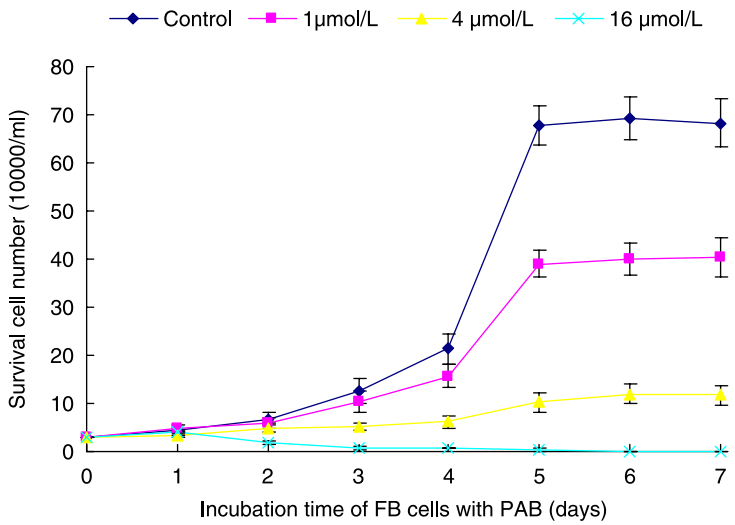

Figure 3. Effect of PLAB on growth of FB cells, FB cells were treated with PLAB (1–16 μmol/L). Values reflect the mean number of cells ± SE for three replicate wells at different intervals.

treated with 1 μmol/L PLAB increased about 20 times. Furthermore, the growth of the group treated with 4 μmol/L PLAB was inhibited on the fifth day. From the beginning, tumour cell growth of the group treated with 16 μmol/L PLAB was inhibited completely.

2.2 PLAB induces apoptosis

PLAB induced morphological changes, which were characteristic of apoptosis in fibroblasts (figure 4). Contrast cells displayed excellent growth characteristics. PLAB evoked typical apoptotic features of cells such as membrane blebbing, cell shrinkage and detachment, and nuclear condensation and fragmentation.

Flow cytometric analysis of fibroblasts exposed to PLAB confirmed the morphological observations above. DNA fluorescence histograms of PI-stained cells showed low DNA stainability of the PLAB-treated, apoptotic cells, which resulted in a distinct, quantifiable region below the G_1 peak. In contrast, the G_1 peak predominated in control cells (figure 5). Quantification of dose dependency was done by monitoring the amount of nuclei with subdiploid DNA content with flow cytometry (figure 6). The percentage of apoptotic cells increased when the concentration of PLAB increased, and a dose dependency was observed.

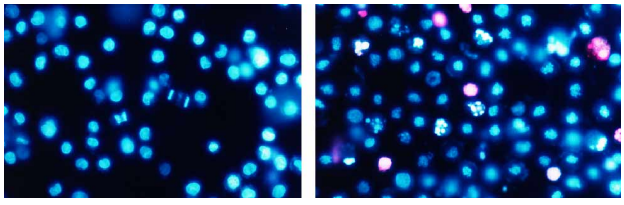

Figure 4. Morphological appearance of cells by fluorescence detection. (A) FB cells treated with 0.1% DMSO; (B) FB cells treated with 16 μmol/L PLAB. P (× 200).

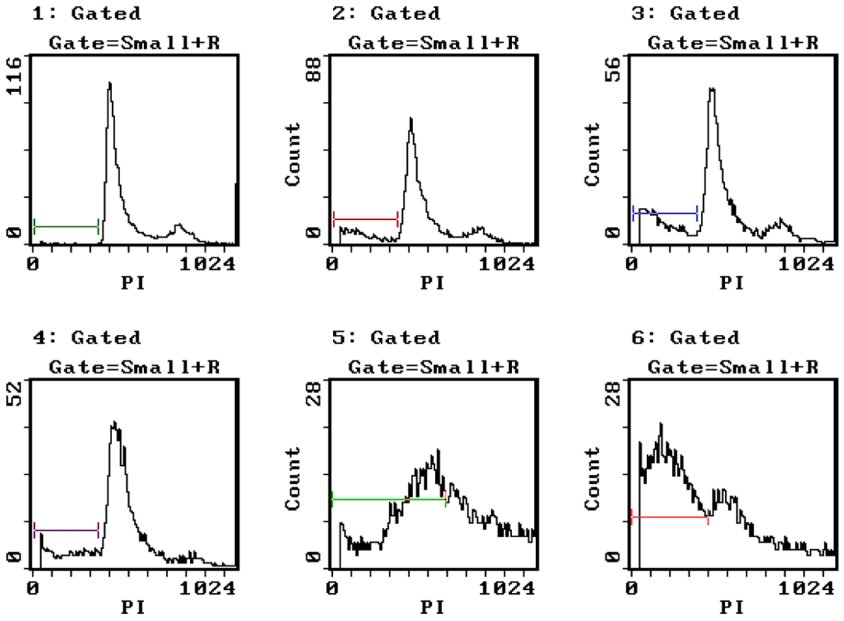

Figure 5. Demonstration of apoptosis by flow cytometric analysis. 1, Untreated FB cells; 2–6, appearance of cells with subdiploid DNA content after exposed to increasing concentrations of PLAB (0.5 μmol/L, 1.0 μmol/L, 2.0 μmol/L, 4.0 μmol/L, 16.0 μmol/L) for 24 h.

Finally, agarose gel electrophoresis showed typical DNA fragmentation pattern of apoptosis (figure 7). DNA fragmentation caused by PLAB was also dose dependent; the intensity of DNA fragments increased when the amounts of PLAB (4–16 μmol/L) were increased.

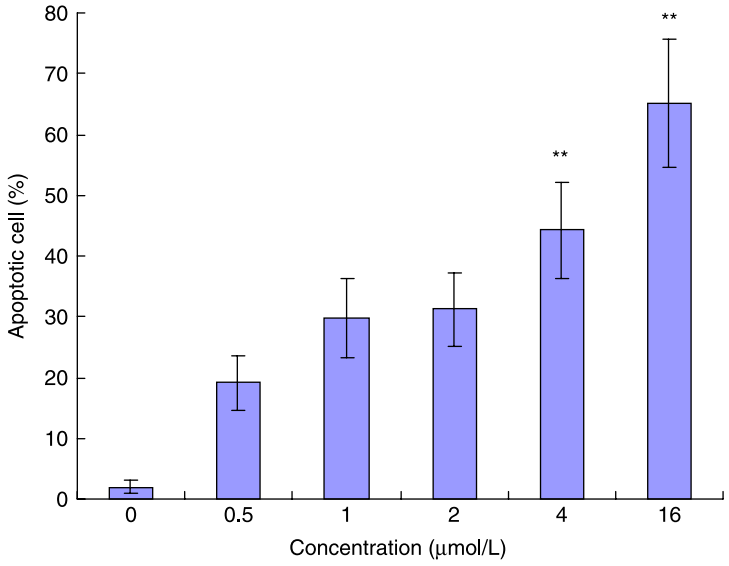

Figure 6. Dose-dependent induction of apoptosis by PLAB. Cells were incubated with increasing concentrations of PLAB for 24 h. % apoptotic cells, percentage of cells with subdiploid DNA content as described under Experimental. Bars, mean ± standard deviation of three experiments performed in triplicate. $^{**}P < 0.01$ (t-test).

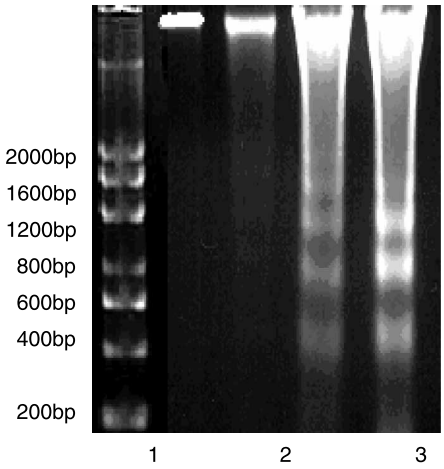

Figure 7. PLAB induced DNA fragmentation in FB cells. DNA was separated and analysed on agarose gel as described in Experimental. Lane 1, DNA size marker; lane 2, FB cells untreated; lanes 3,4,5, FB cells treated with 1 μmol/L, 4 μmol/L, 16 μmol/L. PLAB for 24 h. DNA extracted from FB cells untreated (contr.) or exposed to increasing concentrations of PLAB (1–16 μmol/L) for 24 h was separated by agarose gel (1.8%) and stained with ethidium bromide.

2.3 Effect of PLAB on the expression of Smad2 and Smad7 mRNA of hypertrophic scar fibroblasts

The smad7 mRNA levels when treated by PLAB (2 μmol/L and 4 μmol/L) were (48.80 ± 18.40)% and (65.25 ± 19.40)%, while the corresponding mRNA level was (27.18 ± 13.84)% in the control group (figures 8, 9). There was significant difference in smad7 mRNA expression between the control group and the experimental group ($P < 0.05$), while Smad2 mRNA expression was not significantly different between the two groups (figure 9).

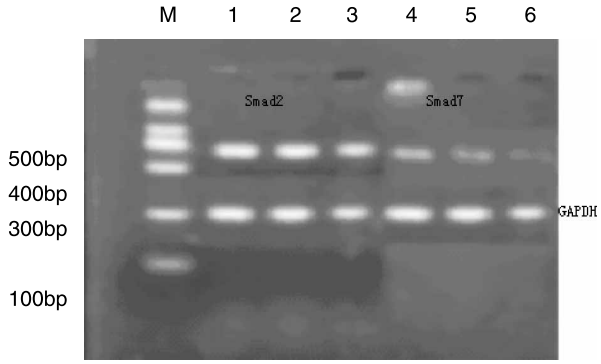

Figure 8. PLAB affects Smad2, Smad7 mRNA expression in FB. FB cells were continuously exposed to PLAB (0.5–2.0 μmol/L) for 24 h, mRNA expression determined by RT-PCR analysis as described under Experimental. 1, expression of control cells treated with 0.1% DMSO smad2 and GAPDH mRNA; 2,3, expression of cells treated with 0.5–2 μmol/L PLAB smad2 and GAPDH mRNA; 4,5, expression of cells treated with 2.0,0.50 μmol/L PLAB smad7 and GAPDH mRNA; 6, expression of control cells treated with 0.1% DMSO smad7 and GAPDH mRNA.

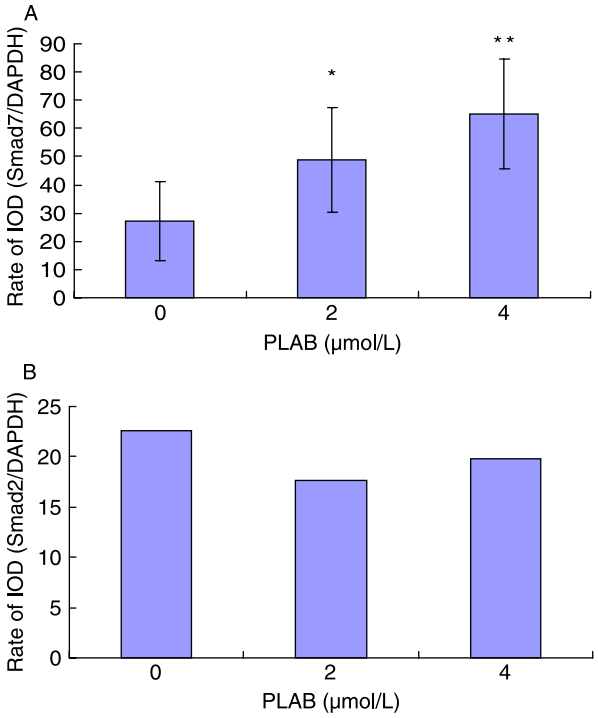

Figure 9. (A) PLAB affects Smad7 mRNA expression in FB. FB cells were continuously exposed to PLAB (0.5–2.0 μmol/L) for 24 h. (B) PLAB affects Smad2 mRNA expression in FB cells were continuously exposed to PLAB (0.5–2.0 μmol/L) for 24 h. *Compared with control group, $P < 0.05$; **compared with control group, $P < 0.01$.

2.4 Effect of PLAB on microtubule organisation

To investigate whether PLAB induces destabilisation of microtubules in a cell-free system, purified tubulin was allowed to polymerise in the absence or presence of different compounds. Increasing concentrations of PLAB led to a progressive decrease in tubulin polymerisation. When PLAB was added to the assay, microtubule protein polymerisation was strongly decreased in a concentration-dependent manner compared with the solvent (DMSO) alone. PLAB also completely blocked tubulin depolymerisation in a concentration-dependent manner. No microtubule polymers could be depolymerised after the addition of PLAB (16 μmol/L) to the assay (figure 10).

2.5 Effect of PLAB on polymerisation of purified tubulin

The effects of PLAB on the microtubule cytoskeleton of FB were investigated by fluorescence microscopy. In untreated FB cells, microtubules formed a fine extensive network throughout the cytoplasm that was generally aligned with the cell axis. By contrast, microtubules in 4 μmol/L PLAB-treated FB began to appear disrupted, in 8 μmol/L, microtubules no longer formed organised bundles, and in 16 μmol/L, microtubules were detected in only a diffuse punctuated pattern (figure 11).

Hypertrophic scar formation is a wound-healing response, which fails to resolve and leads to formation of a raised collagen mass extending beyond the original wound margins. Apoptosis is a form of physiological cell death, characterised by chromatin condensation,

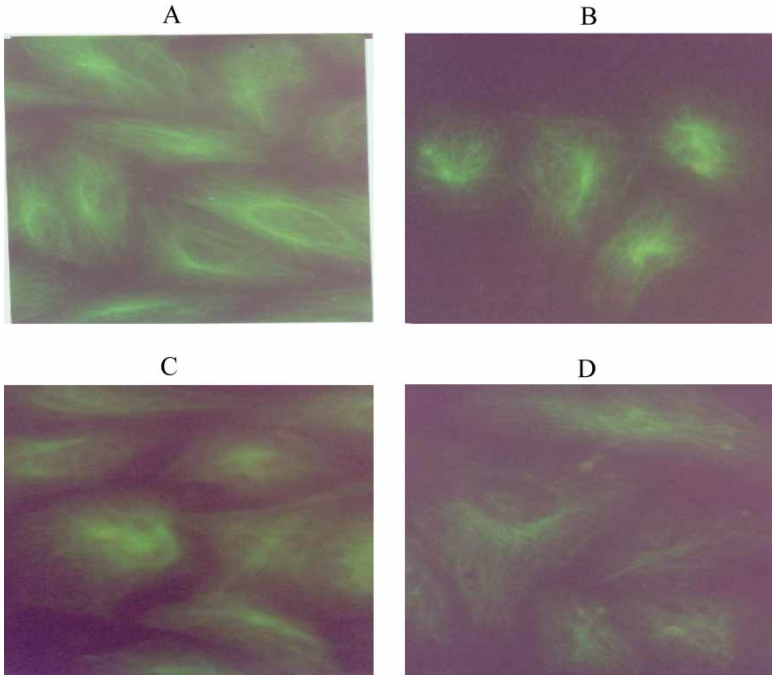

Figure 10. Effect of PLAB on microtubule structures in FB cells. Microtubules were visualised by immunofluorescence with a mouse primary anti-α-tubulin antibody and a species-specific secondary antibody conjugated to FITC (green). The secondary antibody solution also contained Hochest-33342, a DNA binding dye, which was used to visualise nuclear structure (blue). (A) 0.1% DMSO; (B–D) 1.0 μmol/L, 4.0 μmol/L, 16.0 μmol/L of PLAB.

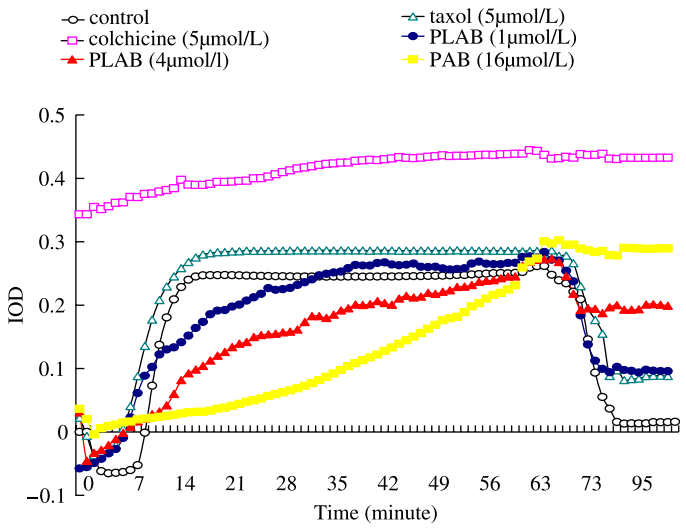

Figure 11. Tubulin polymerisation reactions induced by Taxol, colchicine, and PLAB. (1) 0.1% DMSO (control); (2) Taxol; (3) colchicine; (4)–(6) 1.0 μmol/L, 4.0 μmol/L, 16.0 μmol/L PLAB.

cytoplasmatic blebbing and DNA fragmentation [9]. A dysregulated apoptotic process is involved in the excessive accumulation of extracellular matrix [10]. Fibroblasts are the main effector cells in wound healing process, and can proliferate, migrate, secrete to the extracellular matrix, and differentiate into myofibroblasts. Messadi *et al.* used an Annexin-V–FITC binding assay to show that normal skin fibroblast cultures were found to have a two-fold higher percentage of apoptotic cells than hypertrophic scar fibroblast culture [11]. More evidence showed that development of hypertrophic scar might be related to the decrement of apoptotic fibroblasts [12,13]. Our results showed that PLAB can induce fibroblast apoptosis, and dose dependency was observed.

Microtubules are central to a number of cellular processes including the formation of the mitotic spindle. Indeed it was the destruction of the spindle that led to a loss of chromosome segregation with consequent inhibition of cell division and apoptosis [14]. Our results showed that PLAB interfered with microtubule polymerisation and disrupted the cytoskeleton, which we believe is the mechanism of PLAB-induced FB apoptosis.

More and more evidence has shown that down-regulation TGF-β can inhibit scar hyperplasia. The Smad family, which comprises TGF-β downstream effectors, has been identified in recent years. The Smad family has eight different members. They can be subdivided into three distinct subclasses: (1) Receptor-activated Smads (R-Smads), including Smad1, 2, 3, 5, and 8. Among these, Smad2 and Smad3 are mediators of TGF-β and activate signalling. (2) Common-partner Smads (Co-Smads), including Smad4, which play a critical role in signalling by TGF-β superfamily members. (3) Inhibitory Smads (anti-Smads), including Smad6 and Smad7, which have been characterised as inhibitors of TGF-β signal transduction. Smad7 plays a more pronounced role in inhibition of TGF-β and BMP signalling [15,16]. TGF-β signal transmission starts from heterogenetic dimer formed by TGF-β type I and type II receptors. The activated TGF-β type I receptor induces serine phosphorylation of Smad2/3. Smad2/3 molecule opens and forms a heterodimer with Smad4, which transfers into the nucleus to integrate directly with the specific sequence of TGF-β inducing gene, or to regulate and transcribe indirectly through the mutual action with other nucleus proteins. In the nucleus, the activated Smad2/3 degrades swiftly. At the same time, TGF-β activates Smad7 and brings negative feedback into play so as to break off signal transmission [16]. Our results showed that PLAB increased the expression of inhibitive Smad7 gene in fibroblast, and there was a significant difference between the control group and the experimental group, but there was no significant difference in Smad2 gene between the two groups. Thus it was suggested in this research that PLAB inhibited scar hyperplasia by increasing the expression of inhibitive Smad7 gene in fibroblasts.

In all, our results first showed that PLAB inhibited hypertrophic scar through induced apoptosis of FB and Smad signal pathway. Secondly, PLAB affects the cellular microtubular cytoskeleton of FB.

3. Experimental

3.1 General experimental procedures

Pseudolaric acid-B, provided by Professor Hong Chen, was a white solid with mp 145–146°C, and was >98% pure. It was dissolved in dimethylsulphoxide and further diluted in cell culture medium before use. The final concentration of DMSO in the solution was

$<0.1\%$. It was stored at 4°C before use. Proteinase K, RNase A, SDS Na, acrylamide and Hoechst-33342 were purchased from Sigma Chemical Co. (St Louis, MO, USA). DMEM and trypsin, propidium iodide, Tris and MES were products of Gibco Laboratories (Grand Island, NY, USA). Trizol was purchased from Gibco. Mouse anti-α-tubulin antibody and goat anti mouse IgG/FITC antibody were purchased from Beijing Zhongshan Golden Bridge Biotechnology Co. Ltd.

3.2 Cell culture

We prepared fibroblast cultures from fresh hypertrophic scar tissues obtained. Six patients were included in this study, whose age ranged from 15 to 50 years and among whom three were female. The age of scar proliferation ranged from 3 to 6 months. Tissue culture was adopted and the second-generation cell was applied for the test.

3.3 MTT assay

Cells were detached by trypsinisation, seeded at 2.0×10^3 cells/well in a 96-well microtitre plate overnight, and treated with different concentrations of PLAB in DMEM with 10% foetal bovine serum. The effects on cell growth were examined by MTT assay. Finally, 50 μl of MTT solution (1 mg/ml in DMEM) was added to each well and incubated at 37°C for 4 h. The MTT–formazan formed by metabolically viable cells was dissolved in 150 μl of DMSO, and monitored by a microplate reader at dual-wavelength of 570 and 450 nm, and the IC_{50} values were defined as the drug concentrations that inhibited the cell number to 50% after 96 h. The experiment was repeated three times and the combined data were compared by Student's paired *t*-test.

3.4 Cellular growth curve control

The cells in log phase were trypsinised and seeded in a 25-ml culture flask at a density of 1.5×10^4/ml. Cells from the four groups were digested and counted under inverse light microscope every 24 h for 7 successive days in order to complete the growth curve *in vitro*.

3.5 Assessment of apoptosis by Hoechst and PI staining

To analysis chromatin condensation, which is a sign of apoptosis, 1×10^4 cells were added to each well of the 24-well plates. Cells were exposed to PLAB (8 μmol/L) for 24 h, and then Hoechst and PI staining were performed. Final concentration of Hoechst-33342 was 5–10 μg/ml and the final concentration of PI was 50 μg/ml. At first 4% formaldehyde solution was added to each well in which cells had been exposed to PLAB. The cells were then incubated with the dilute Hoechst-33342 and PI solution for 10 min at room temperature. Finally, each well was examined under a fluorescence microscope equipped with a DM455 filter for chromatin condensation.

3.6 Assessment of apoptosis by flow cytometry

Trypsinised cells were washed with PBS and then fixed with 70% ethanol. The fixed cells were kept overnight at −20°C. The cells were washed with PBS before analysis, and then

the fluorochrome solution (50 μg/ml propidium iodide in PBS, plus RNase, 50 μg/ml) was added. Distribution of the cell cycle phases was determined by analytical flow cytometry using a Coulter Epics XL (Coultronics, France) with an excitation/emission of 488/525 nm. All experiments were performed three times.

3.7 Assessment of apoptosis by DNA fragmentation

Cells incubated with PLAB (4–16 μmol/L) for 24 h were collected and washed two times in PBS, then resuspended in 0.5 ml of extraction buffer (100 mmol/L NaCl, 10 mmol/L Tris–HCl pH 8.0, 25 mmol/L EDTA pH 8.0, 0.1 mg/ml Proteinase K) at 50°C for 12 h. DNA was extracted with an equal volume of phenol saturated/chloroform/isoamyl alcohol (25:24:1) and extracted again with a combination of chloroform/isoamyl alcohol (24:1), then centrifuged at 12,000 × *g* for 30 min. Precipitated DNA was analysed on a 2.0% agarose gel.

3.8 RT-PCR analysis

Total RNA was isolated from cells using Trizol Reagent (Gibco). After denaturing (94°C, 5 min), 500 ng of RNA was transcribed into cDNA which was amplified using the following primers: sense hSmad2 (5′-ATG CCA CGG TAG AAA TGA C-3′), antisense hSmad2 (5′-TTG AGC AAC GCA CTG AAG G-3′), sense hSmad7 (5′-AGC AGA AAT CCA AGC ACC-3′) and antisense hSmad7 (5′-CTG GCA GGA AGG GAA TAA G-3′), sense hGAPDH (5′-CGT CTT CAC CAC CAT GCA GA-3′) and antisense hGAPDH (5′-CGG CCA TCG CCA CAG TTT-3′). Duplex amplification was performed using a thermocycler for 30 cycles according to the following programme: 1 min at 95°C, 30 s at 50°C, and 1 min at 72°C. PCR fragments were separated electrophoretically in 1% agarose gel, with hGAPDH (300 bp) as an internal standard. The band intensity was determined from scanned images using Gel-Pro Analyser 3.1 Automated Digitising System software. Each experiment was repeated three times and the combined data were compared by Student's paired *t*-test.

3.9 Indirect immunofluorescence microscopy

Cells were incubated for 24 h with PLAB (4–16 μmol/L) and then were rinsed by PEMP (0.1 M PIPES [1,4-piperazinediethanesulfonic acid], 4%PEG [polyethylene glycol]-8000, 1 mM EGTA [ethylene glycol bis(β-aminoethyl ether)-*N*,*N*,*N*′,*N*′-tetra-acetic acid], 1 mM MgCl); the cells were treated with 0.5% Triton X-100/PEMP at 37°C. The cultures were fixed in 3.7% formaldehyde/PEMD solution for 30 min, then incubated with the primary monoclonal anti-α-tubulin antibody diluted 1:500 in 0.1% bovine serum albumin in PBS at 37°C for 2 h. After extensive washings in cold PBS, the cells were incubated with the secondary antibody goat anti mouse IgG/FITC antibodies diluted 1:500 at 37°C for 2 h. The cells were washed in PBS and mounted with glycerol using glass coverslips. Cells were studied by fluorescence microscopy [9].

3.10 Tubulin polymerization–depolymerisation assay

Purified tubulin from swine brain were abstracted according to Robley's method [10]. Tubulin heterodimers (10 μmol/L) were incubated with PLAB (4–16 μmol/L), Taxol

(5 μmol/L) and colchicine (5 μmol/L) in PEMP buffer containing 1 mM ATP in a total volume of 200 μl at 0°C (icewater bath). Then the temperature of the microplate reader was set at 37°C. Samples were moved from icewater to microplate reader and every half minute the OD of samples were recorded at wavelength of 350 nm for 20 min. the temperature of the microplate reader was then set to 0°C, and every half minute OD of samples were recorded at wavelength of 350 nm for 20 min. The curve of tubulin polymerization–depolymerisation was plotted.

References

[1] S.P. Yang, Y. Wang, Y. Wu, J.M. Yue. *Nat. Prod. Res.*, **58**, 57 (2004).
[2] S.P. Yang, Y. Wang, Y. Wu, J.M. Yue. *J. Nat. Prod.*, **65**, 1041 (2002).
[3] Y.L. Zhang, R.Z. Lu, A.L. Yan. *Zhongguo Yao Li Xue Bao*, **11**, 60 (1990).
[4] S.P. Yang, L. Dong, Y. Wang, Y. Wu, J.M. Yue. *Bioorg. Med. Chem.*, **11**, 4577 (2003).
[5] B. Liu, H. Chen, Z.Y. Lei, P.F. Yu, B. Xiong. *Planta*, **56**, 383 (2006).
[6] V.K. Wong, P. Chiu, S.S. Chung, L.M. Chow, Y.Z. Zhao, B.B. Yang, B.C. Ko. *Clin. Cancer Res.*, **86**, 6002 (2005).
[7] C. Linge, J. Richardson, C. Vigor. *J. Invest. Dermatol.*, **125**, 72 (2005).
[8] T. Chodon, T. Sugihara, H.H. Igawa, E. Funayama. *Am. J. Pathol.*, **157**, 1661 (2000).
[9] D.T. Loo, J.R. Rillema. *Methods Cell Biol.*, **57**, 251 (1998).
[10] A. Burd, L. Huang. *Plast. Reconstr. Surg.*, **116**, 150 (2005).
[11] D.V. Messadi, A. Le, S. Berg, A. Jewett, Z. Wen, P. Kelly, C.N. Bertolami. *Wound Repair Regen.*, **7**, 511 (1999).
[12] A. Nakazono-Kusaba, F. Takahashi-Yanaga, Y. Miwa, S. Morimoto, M. Furue, T. Sasaguri. *Eur. J. Pharmacol.*, **497**, 155 (2004).
[13] T. Chodon, T. Sugihara, H.H. Igawa, E. Funayama, H. Furukawa. *Am. J. Pathol.*, **157**, 1661 (2000).
[14] C.L. Rieder, H. Maiato. *Dev. Cell.*, **7**, 637 (2004).
[15] J. Massague. *Annu. Rev. Biochem.*, **67**, 753 (1998).
[16] E. Piek, C.H. Heldin, P. Ten Dijke. *FASEB J.*, **13**, 2105 (1999).